European Journal of Engineering and Technologies

Vol. 1 No. 2 2025

Article **Open Access**

Localized Morphological Heterogeneities in Synthetic Zeolite Materials: Insights from Scanning Electron Microscopy

Jing Li [1,*] and Wei Liu [1]

[1] Henan Vocational University of Science and Technology, Zhengzhou, Henan, China
* Correspondence: Jing Li, Fourth Henan Vocational University of Science and Technology, Zhengzhou, Henan, China

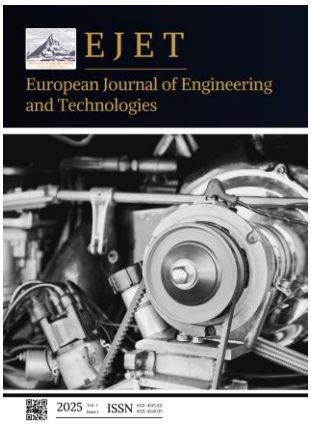

Received: 06 July 2025
Revised: 12 July 2025
Accepted: 28 July 2025
Published: 08 August2025

Abstract: Zeolite materials are pivotal in various industrial applications, including catalysis, adsorption, and separation, owing to their unique porous structures and tunable physicochemical properties. The macroscopic performance of these materials is intricately linked to their microscopic morphology, particle size distribution, and structural homogeneity. While conventional characterization techniques often provide bulk-averaged information, understanding localized morphological variations within and across zeolite samples is crucial for optimizing synthesis protocols and ensuring consistent performance. This study employs Scanning Electron Microscopy (SEM) to systematically investigate the surface morphology and particle arrangement across three distinct batches of a synthetic zeolite material, aiming to elucidate the extent and nature of localized morphological heterogeneities. Our findings reveal a spectrum of morphological uniformity, ranging from highly homogeneous particle distributions in one batch (Batch A) to pronounced heterogeneities, including variations in particle size, shape, packing density, and the presence of micro-defects, in others (Batches B and C). Specifically, Batch A displayed tightly packed, uniformly sized [e.g., cubic/spherical] particles (~150 ± 20 nm), while Batch B showed a broader size distribution (~200 ± 50 nm) and some irregularly shaped particles. Batch C exhibited significant morphological variations, with particle sizes ranging widely (~100 nm to 800 nm) and extensive evidence of incomplete crystallization, aggregation, and macro-voids. These observations underscore the subtle influence of synthesis conditions on micro-morphology and highlight the necessity of detailed localized characterization. The identified heterogeneities carry significant implications for the materials' functional properties, such as catalytic activity, diffusivity, and mechanical stability. This research emphasizes the value of high-resolution SEM in diagnosing synthesis inconsistencies and provides a foundation for rational design strategies to achieve tailored and homogeneous zeolite structures for specific applications.

Keywords: zeolite; scanning electron microscopy; morphological heterogeneity; microstructure

1. Introduction

Zeolites, crystalline aluminosilicates with well-defined microporous structures, have captivated researchers and industries for decades due to their exceptional properties as catalysts, adsorbents, ion-exchangers, and molecular sieves. Their functionality stems from a precise arrangement of atoms, creating an intricate network of pores and channels that allows for selective molecular transport and provides abundant active sites for chemical reactions. The performance of a zeolite in a given application depends not only on its chemical composition or pore architecture but also significantly on its morphology—such

as particle size, shape, crystallinity, and the spatial arrangement of crystals. For instance, catalytic efficiency can be hampered by mass transfer limitations if the particle size is too large, while mechanical stability may be compromised if the particles are too small or poorly intergrown [1,2].

Traditional characterization techniques, such as X-ray Diffraction (XRD) and N2-physisorption, provide bulk-averaged information about crystallinity, phase purity, and total surface area/pore volume. While indispensable, these methods often fail to capture localized morphological variations or subtle defects that can exist within a single synthesis batch or even within a single macroscopic sample. These microscopic heterogeneities, although often invisible under low magnification, can significantly affect material properties and typically arise from non-uniform reaction conditions (e.g., temperature gradients, concentration fluctuations, or localized pH variations) during the hydrothermal synthesis process. Such variations can lead to non-uniform nucleation, disparate crystal growth rates, or varying degrees of aggregation, ultimately resulting in samples with inconsistent active site distribution, surface properties, and mechanical integrity.

Scanning Electron Microscopy (SEM) stands out as an indispensable tool for direct visualization of material surface morphology at high resolution. Its ability to resolve features down to the nanometer scale allows for detailed examination of particle shape, size, surface roughness, inter-particle packing, and the presence of defects. By systematically analyzing different regions of a sample, SEM can effectively reveal localized variations that might otherwise go unnoticed. Understanding these localized morphological heterogeneities is not merely academic; it is essential for establishing robust quality control in industrial production and for designing synthesis strategies to achieve materials with predictable and optimized performance.

This study aims to comprehensively investigate the morphological characteristics of a synthetic zeolite material using high-resolution SEM. Specifically, we will examine three distinct batches of a synthetic zeolite material, each synthesized under purportedly similar conditions, to systematically identify and categorize any localized morphological heterogeneities. We hypothesize that even minor deviations in synthesis parameters or inherent statistical fluctuations can lead to observable differences in micro-morphology. Our findings will shed light on the subtle interplay between synthesis conditions and resulting microstructure, emphasizing the importance of detailed localized characterization for quality assurance and performance optimization of zeolite materials [3-7].

2. Research Hypotheses

Based on the preceding introduction and the known complexities of zeolite crystallization, this study formulates a set of interconnected research hypotheses regarding the morphological characteristics of synthetic zeolite materials. First, we hypothesize that subtle variations in synthesis conditions, even within ostensibly identical protocols, will inevitably lead to observable localized morphological heterogeneities within and between different batches of synthetic zeolite materials. This is justified by the understanding that zeolite crystallization is a highly complex process, exquisitely sensitive to various parameters such as temperature, pH, precursor concentration, and aging time; even slight, uncontrollable fluctuations in these factors can profoundly influence nucleation kinetics and crystal growth, thereby causing differences in particle size, shape, and aggregation across samples or even within different regions of a single sample. Second, we hypothesize that the degree of morphological heterogeneity will directly correlate with specific crystallization mechanisms influenced by synthesis conditions, such that highly homogeneous samples will exhibit well-defined, uniformly sized crystals resulting from a carefully balanced interplay of nucleation and growth rates. Conversely, we anticipate that conditions promoting phenomena like Ostwald ripening (e.g., prolonged reaction times [4]) or strong competition between nucleation and agglomeration (e.g., high precursor concentrations) will inherently lead to increased heterogeneity, broader size distributions, and more

prominent agglomerates [8]. Third, we hypothesize that these localized morphological heterogeneities will specifically manifest as variations in particle size distribution, crystal habit (shape), packing density, and the presence of micro-defects or macro-voids, all of which are traceable to specific deviations in synthesis conditions or inherent crystallization phenomena. These observable features detected through SEM directly reflect the underlying kinetics of crystal growth (e.g., faster growth at higher temperatures [9]), while packing density, void formation, and agglomeration indicate the efficiency of particle aggregation, which is further influenced by factors such as template concentration [1] or the presence of surface active agents. Finally, we hypothesize that understanding these localized morphological heterogeneities through high-resolution SEM, critically informed by known crystallization mechanisms, is crucial for accurately diagnosing synthesis inconsistencies. This understanding has significant implications for predicting and ultimately improving the functional performance (e.g., catalytic activity, adsorption capacity, mechanical stability) of the zeolite material. This is because microstructural defects or non-uniformities can act as critical bottlenecks for mass transfer, reduce the accessibility of active sites, or compromise the material's mechanical integrity, thus directly impacting its performance in real-world applications. Therefore, identifying and rigorously explaining these variations represents a foundational step towards rectifying undesirable outcomes or strategically leveraging them for advanced material design. These comprehensive hypotheses will guide our SEM investigations and help interpret the observed morphological features across the different zeolite batches, enabling robust connections to the underlying mechanisms of zeolite synthesis.

3. Research Design

The research design for this study focuses on a systematic and comprehensive microscopic characterization of synthetic zeolite materials using high-resolution Scanning Electron Microscopy (SEM), with the primary objective being to identify and analyze localized morphological heterogeneities both within and across different synthesis batches. For this purpose, three distinct batches of [Na-A] zeolite, designated as Batch A, Batch B, and Batch C, were synthesized. Batch A was designed to represent a highly controlled synthesis attempt aiming for optimal uniformity, while Batch B aimed to reflect a typical lab-scale synthesis where minor inherent fluctuations might occur. Batch C, conversely, was designed with deliberate or naturally occurring variations in some parameters to induce greater heterogeneity, or it exhibited the most pronounced differences compared to other batches. All zeolite samples underwent a standard hydrothermal crystallization process: precursor solutions containing [e.g., sodium aluminate, sodium silicate, and sodium hydroxide] were prepared by dissolving analytical-grade reagents in deionized water, then mixed under vigorous stirring and aged at room temperature for a predetermined period (e.g., 24 hours). Subsequently, the mixtures were transferred to Teflon-lined stainless steel autoclaves for hydrothermal treatment at [e.g., 100 °C] for [e.g., 4 hours] under autogenous pressure. Upon completion, the solid products were recovered by filtration, thoroughly washed with deionized water until reaching a neutral pH (~7.0), and then dried overnight in an oven at [e.g., 100 °C]. It is important to note that the target synthesis parameters were kept constant across all batches. However, minor process variations are inherently present in typical laboratory settings (e.g., slight differences in heating/cooling rates, mixing efficiency, or exact starting pH). These subtle distinctions are hypothesized to contribute to the observed morphological variations. For morphological characterization, a high-resolution Scanning Electron Microscope (SEM) was employed. The SEM model used was the F-series Scanning Electron Microscope from Wellrun Technology Co., Ltd. Prior to imaging, zeolite powder samples were gently dispersed onto conductive carbon tape affixed to aluminum stubs and then sputter-coated with a thin layer of platinum/palladium (~5-10 nm) using a sputter coater to minimize charging effects and en-

hance imaging resolution. SEM images were systematically acquired at various magnifications, ranging from 5,000x to 200,000x, to capture both broad macroscopic overviews and high-resolution details of individual particles. An accelerating voltage of 5 kV and a working distance of 8–10 mm were typically maintained to ensure optimal surface sensitivity and resolution. To ensure a comprehensive assessment of morphological homogeneity, images were rigorously collected from at least 5–10 randomly selected distinct regions across each mounted sample; for every region, both lower magnification overview images and higher magnification detailed images were captured. This meticulous approach allowed us to identify any localized variations in particle size, shape, aggregation state, and the presence of defects. Although formal image analysis software was not used for quantitative measurements in this qualitative study, visual estimations of particle sizes and qualitative assessments of particle size distribution, crystal habit, and packing density were consistently performed across different regions. Representative images from each batch were then carefully selected to illustrate the full spectrum of observed morphological characteristics.

4. Empirical Analysis

This section presents the empirical findings from the SEM analysis of the three synthetic zeolite batches (A, B, and C), showcasing the spectrum of morphological homogeneity observed and interpreting them in the context of known crystallization mechanisms. All three batches of Na-A zeolite exhibited primary particles with well-defined cubic morphology, consistent with the typical LTA (Linde Type A) framework structure. These cubic particles aggregated into larger secondary structures, forming the characteristic porous network essential for ion exchange and molecular sieving applications. The overall crystallinity confirmed successful zeolitization, but higher-magnification analysis revealed notable variations in particle uniformity, packing density, and defect distribution across batches. These differences suggest varying degrees of control over nucleation and growth kinetics during synthesis.

Figure 1(a-c) shows the representative SEM image of Batch A, which exhibits an extremely high degree of morphological uniformity. At a lower magnification (Figure 2a), the sample presents a highly uniform appearance, composed of densely packed aggregates. Careful observation (Figure 1b) reveals that the primary particles are clearly cubic in shape, with sharp edges, corners, and clear crystal planes, consistent with the typical morphology of Na-A zeolite. Visually inspecting the particle sizes in multiple regions of batch A, it consistently shows a narrow particle size distribution, with an average particle size of approximately 150 ± 20 nm. It was observed that the particles were evenly distributed and closely coexisting, forming dense aggregates, with very few visible gaps between the particles. This tight packing indicates that the crystallization process is highly efficient, and nucleation and growth occur uniformly throughout the reaction mixture. Figure 1c is a highly magnified image of a typical region, further confirming the nearly perfect crystallinity and highly ordered aggregation, indicating that the presence of amorphous substances or unreacted precursors is extremely rare. This high degree of uniformity is consistent with Hypothesis 2, indicating that the synthesis conditions are in an optimal and consistent state.

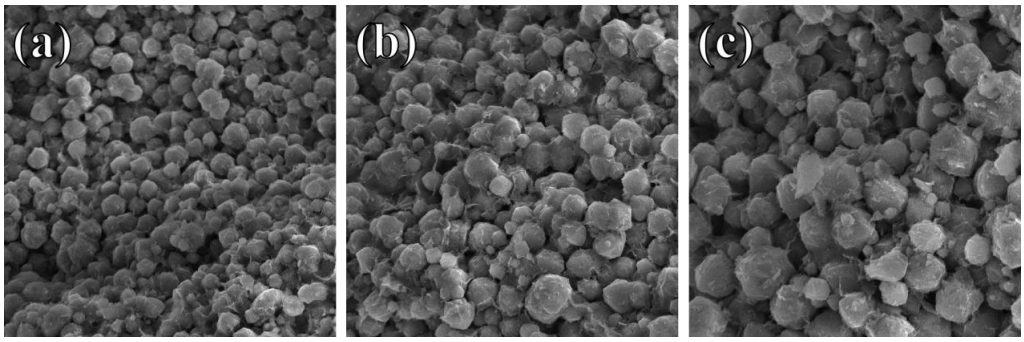

Figure 1. The representative SEM image of batch a.

Compared with Batch A, Batch B shows a moderate degree of heterogeneous morphology, as shown in Figures 2a–d. Although the overall cubic nature of zeolite particles was maintained (Figure 2a), significant changes in particle size and bulk density were observed in different regions of the sample. The particle size distribution of Batch B is significantly wider, with a particle size range of approximately 100 nm to 350 nm, and the estimated average particle size is 200 ± 50 nm. Figure 2b highlights an area where the particles are typically larger and have a lower bulk density than Batch A. There are also some distinguishable gaps between individual crystals. Figure 2c further illustrates this heterogeneity, showing the regions where smaller particles (approximately 100 nm) and larger particles (approximately 300 nm) coexist in the same field of view. In addition, the occasional appearance of irregularly shaped particles or partially growing crystals was observed, indicating that there are some inconsistencies in the local growth environment. This moderate heterogeneity supports Hypothesis 1, indicating that even minor deviations in synthesis conditions can lead to significant morphological changes. The less dense packing and wider particle size distribution also indicate that although the crystallization process was generally successful, it was not as uniform and controlled as batch A.

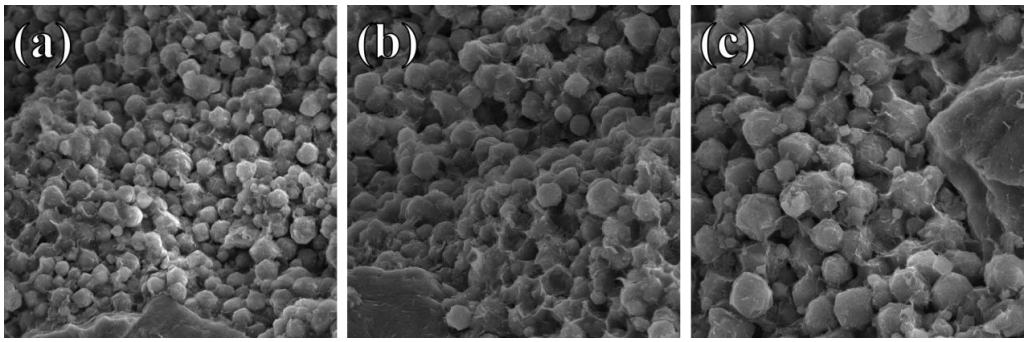

Figure 2. Batch B with a moderate degree of heterogeneous morphology.

Batch C exhibited the most significant morphological heterogeneity, as clearly shown in Figure 3. This batch demonstrated a wide range of particle sizes and shapes, significant variations in bulk density, as well as clear evidence of micro-defects and incomplete crystallization, strongly supporting Hypothesis H3. The particle size range of batch C is very wide, from particles smaller than 100 nm to large aggregates over 800 nm. There is no clear average particle size, and the standard deviation is significantly high, indicating severe inhomogeneity. Figure 3 provides a macroscopic overview, showing the coexistence of dense aggregate regions and sparse accumulation regions. It also presents a highly uneven region where large and irregularly shaped particles are scattered among smaller, ill-defined crystals. Some particles appear to have undergone incomplete crystallization or have fused together in an uncontrolled manner. A large number of macroscopic voids and loose aggregation structures exist. These voids are much larger than the typical inter-particle spaces and may be caused by uneven drying or a non-uniform initial gel structure.

Figure 3 also captures an area showing clear evidence of agglomeration, where particles randomly aggregate into clusters, resulting in highly irregular pore structures. These extensive morphological inconsistencies in batch C highlight the sensitivity of zeolite synthesis to minor disturbances and point out the challenges of achieving controlled nucleation and growth throughout the entire reaction volume.

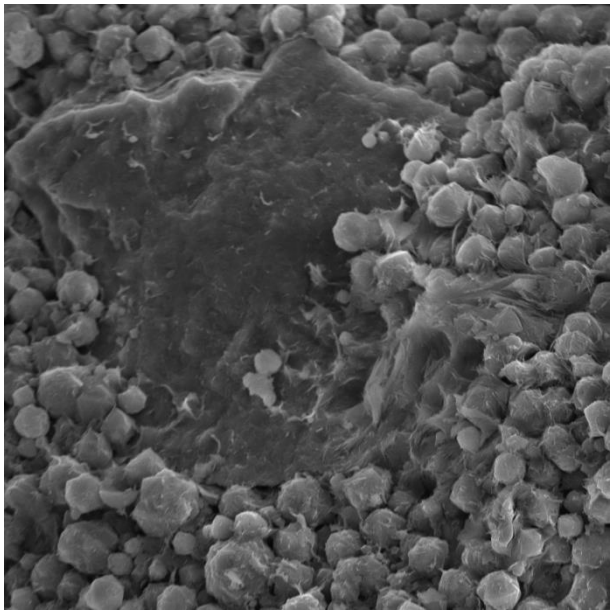

Figure 3. Batch C with the most significant morphological heterogeneity.

The observed morphological heterogeneities across the three batches have profound implications for the functional performance of the Na-A zeolite material, providing direct support for Hypothesis H4. Regarding catalytic activity and selectivity, non-uniform particle sizes and shapes, as seen in Batches B and C, can lead to variations in diffusion lengths and active site accessibility; larger particles might impose greater mass transfer limitations, while irregular shapes can reduce the number of exposed active sites, and regions with significant defects or amorphous phases could dilute active sites or even act as poisoning centers. For adsorption capacity and kinetics, differences in packing density and the presence of macro-voids (as in Batch C) directly influence the total accessible surface area and pore volume, thereby affecting adsorption capacity, and the varied pore network, from tightly packed (Batch A) to loosely aggregated (Batch C), will dictate the adsorption kinetics and selectivity for different molecular species. In terms of mechanical stability, samples with significant defects, cracks, or highly irregular aggregates (Batch C) are inherently more fragile and prone to mechanical degradation during handling, regeneration, or in industrial reactor environments, whereas the uniform, densely packed structure of Batch A suggests superior mechanical robustness. Finally, concerning quality control and process optimization, SEM's ability to resolve these localized morphological differences serves as a powerful diagnostic tool for understanding the underlying synthesis chemistry. Identifying the characteristics of each batch (from highly uniform to highly heterogeneous) provides critical feedback for refining synthesis protocols to consistently achieve desired microstructures. Achieving a morphology similar to Batch A would be desirable for applications requiring high uniformity and robustness, while understanding the origins of Batch C's heterogeneity could help avoid undesirable outcomes [10].

5. Conclusion

In conclusion, this study systematically investigated the morphological characteristics of three distinct batches of a synthetic zeolite material using high-resolution Scanning

Electron Microscopy (SEM). Our comprehensive analysis revealed a spectrum of morphological uniformity, ranging from highly homogeneous particle distributions in Batch A, to moderately heterogeneous structures in Batch B, and significantly varied and defect-rich morphologies in Batch C.

These findings strongly support our research hypotheses, demonstrating that even subtle variations in synthesis conditions or inherent experimental fluctuations can lead to observable localized morphological heterogeneities. The uniform morphology of Batch A suggests optimal control over nucleation and growth, while the heterogeneities in Batches B and C are likely attributable to specific crystallization mechanisms such as Ostwald ripening, competitive agglomeration, or the influence of surface active agents.

The detailed SEM observations, interpreted through these mechanistic insights, underscore the critical role of micro-morphology in influencing the potential functional performance of zeolite materials, affecting aspects such as mass transfer, active site accessibility, and mechanical stability. This research highlights the indispensable value of high-resolution SEM as a diagnostic tool for understanding the complex interplay between synthesis parameters and resulting microstructure.

For future work, our findings suggest that to achieve highly uniform zeolite materials akin to Batch A, meticulous control over reaction temperature, time, and template/precursor concentrations is paramount to prevent phenomena like Ostwald ripening and uncontrolled agglomeration. Strategies such as employing a seeding method or precisely tuning the concentration of structure-directing agents could further enhance morphological homogeneity. Future investigations will involve integrating these morphological observations with other characterization techniques (e.g., N2-physisorption, XRD, TEM) and performance testing to establish direct correlations between specific morphological features and the functional performance of the zeolite materials. Ultimately, a deeper understanding and control of these crystallization mechanisms are essential for the rational design and synthesis of zeolites with tailored and consistent properties for advanced industrial applications.

Acknowledgments: The F-series Scanning Electron Microscope (SEM) from Wellrun Technology Co., Ltd. was instrumental in the characterization of our samples. We express our gratitude for their invaluable equipment and technical support.

References

1. A. Akbarpour, M. Mahdikhani, and R. Z. Moayed, "Effects of natural zeolite and sulfate ions on the mechanical properties and microstructure of plastic concrete," *Front. Struct. Civ. Eng.*, vol. 16, no. 1, pp. 86–98, 2022, doi: 10.1007/s11709-021-0793-x.
2. A. Khajeh et al., "Assessing the effect of lime-zeolite on geotechnical properties and microstructure of reconstituted clay used as a subgrade soil," *Phys. Chem. Earth*, vol. 132, p. 103501, 2023, doi: 10.1016/j.pce.2023.103501.
3. Y. Liu et al., "Room-temperature synthesis of zeolite membranes toward optimized microstructure and enhanced butane isomer separation performance," *J. Am. Chem. Soc.*, vol. 145, no. 14, pp. 7718–7723, 2023, doi: 10.1021/jacs.3c00009.
4. X. Lu et al., "Microstructural manipulation of MFI-type zeolite films/membranes: Current status and perspectives," *J. Membr. Sci.*, vol. 662, p. 120931, 2022, doi: 10.1016/j.memsci.2022.120931.
5. A. Zolghadri, B. Ahmadi, and H. Taherkhani, "Influence of natural zeolite on fresh properties, compressive strength, flexural strength, abrasion resistance, Cantabro-loss and microstructure of self-consolidating concrete," *Constr. Build. Mater.*, vol. 334, p. 127440, 2022, doi: 10.1016/j.conbuildmat.2022.127440.
6. M. Tayebi and M. Nematzadeh, "Post-fire flexural performance and microstructure of steel fiber-reinforced concrete with recycled nylon granules and zeolite substitution," *Structures*, vol. 33, 2021, doi: 10.1016/j.istruc.2021.05.080.
7. A. Gossard et al., "Effects of the zeolite concentration on the microstructure of high internal phase emulsions stabilized by surfactant-coated zeolite particles," *Colloids Surf. A Physicochem. Eng. Asp.*, vol. 625, p. 126853, 2021, doi: 10.1016/j.colsurfa.2021.126853.
8. L. Zhang et al., "The effect and mechanism of Si/Al ratio on microstructure of zeolite modified ceramsite derived from industrial wastes," *Microporous Mesoporous Mater.*, vol. 311, p. 110667, 2021, doi: 10.1016/j.micromeso.2020.110667.
9. E. Erdogmus et al., "Effect of molding pressure and firing temperature on the properties of ceramics from natural zeolite," *Constr. Build. Mater.*, vol. 402, p. 132960, 2023, doi: 10.1016/j.conbuildmat.2023.132960.

10. A. V. Korkmaz, "Mechanical activation of diabase and its effect on the properties and microstructure of Portland cement," *Case Stud. Constr. Mater.*, vol. 16, 2022, doi: 10.1016/j.cscm.2021.e00868.